

Improving Generative Pre-Training: An In-depth Study of Masked Image Modeling and Denoising Models

Hyesong Choi¹, Daeun Kim¹, Sungmin Cha², Kwang Moo Yi³, Dongbo Min^{1†}
¹Ewha W. University ²New York University ³University of British Columbia

Abstract

In this work, we dive deep into the impact of additive noise in pre-training deep networks. While various methods have attempted to use additive noise inspired by the success of latent denoising diffusion models, when used in combination with masked image modeling, their gains have been marginal when it comes to recognition tasks. We thus investigate why this would be the case, in an attempt to find effective ways to combine the two ideas. Specifically, we find three critical conditions: corruption and restoration must be applied within the encoder, noise must be introduced in the feature space, and an explicit disentanglement between noised and masked tokens is necessary. By implementing these findings, we demonstrate improved pre-training performance for a wide range of recognition tasks, including those that require fine-grained, high-frequency information to solve.

1. Introduction

Foundational models [11, 23] have appeared as effective solutions to various problems [2, 3, 30, 43, 45]. However, these models are immense and notoriously data-hungry, requiring vast amounts of labeled data to reach their full potential. For example, Stable Diffusion [31] is trained on 400 million images from the LAION-400m dataset [33], and CLIP [28] also with 400 million images. Naturally, to alleviate this data constraint, pre-training of these models that are task-agnostic based on self-supervision [1, 4, 12–14, 40] has drawn interest from the research community.

A popular trend is based on masked image modeling (MIM) [1, 14, 40], thanks to their simplicity and effectiveness. These models mask parts of images and learn feature representations by learning to reconstruct them. While effective, these masked image models primarily capture low-frequency semantics of the scene [14], with the masking and reconstruction process encouraging the model to focus on the general structure and contextual patterns. As

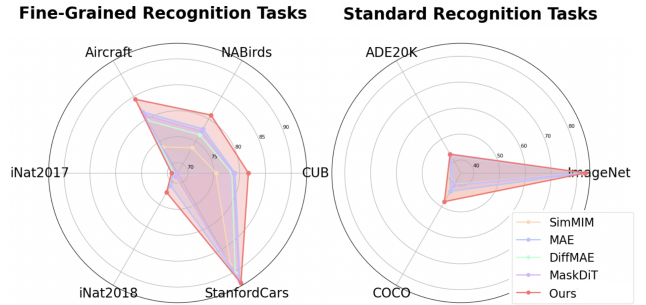


Figure 1. We find that noise-based pre-training, when applied in the right way, can enhance transfer learning ability. Leveraging the insights, we introduce a novel pre-training setup combining masking and noising, outperforming MIM baselines [14, 40] and recent noise-based generative approaches [39, 42] across a wide range of recognition tasks, including fine-grained recognition.

a result, they perform poorly on tasks that require high-frequency details of images, such as fine-grained recognition, as shown in Fig. 1 and later in our experiments.

In other branches of computer vision [29, 31, 32], latent denoising diffusion models have shown to be effective in capturing high-frequency details. These approaches, in particular, excel at generating images and videos with high fidelity. This demonstrates that the latent representations employed by these models must contain high-frequency textures they generate—a potential for downstream tasks that demand fine-grained details [20, 26, 35–38].

Naturally, there have been attempts to utilize the potential of denoising models, by incorporating their ‘noising’-based training to pre-training of deep features. That is, learning to denoise similarly to how masked image models learn to recover images, or even learning to perform both together. For example, Diffused Masking strategy [39] uses tokens with noise added alongside clean ones, replacing the conventional strategy of masking tokens. The hybrid Masking [42] combines masking and noising, by utilizing both masked tokens and noisy visible tokens within its framework. Both of them, however, do not provide notable gains over conventional masking-based approaches to recognition benchmarks [9, 21, 44], as well as in fine-grained recogni-

[†] Corresponding author: dbmin@ewha.ac.kr

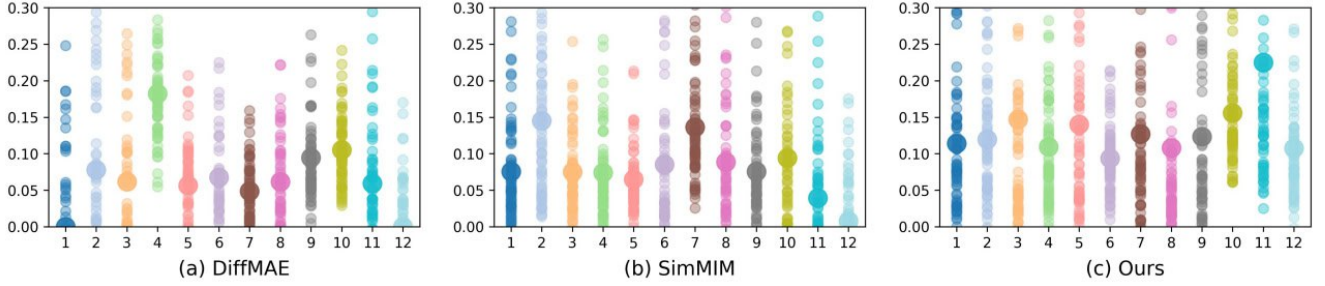


Figure 2. We display the KL divergence among attention distributions across different heads (indicated by small dots) and the mean KL divergence (represented by large dots) in each layer for (a) a recent generative model [39], (b) a representative masked image model [40], and (c) our method. This assesses whether various attention heads capture diverse frequency information, where higher KL divergence indicates broader frequency capture. Our method demonstrates a greater capacity for capturing diverse frequency information than MIM and generative approaches, which explains why it performs well across a wide range of recognition tasks, including fine-grained tasks.



Figure 3. We visualized the self-attention maps for the image classification token in the final layer of our model on a fine-grained visual categorization benchmark. The proposed method captures a range of frequencies by focusing effectively on both key features and fine details within complex scenes.

tion [20, 26, 35–38]; see Fig. 1.

In this paper, we dive deep into why this framework shows limited gains in recognition tasks and discover that it is possible to benefit from noise-based pre-training, much like the denoising diffusion models, *if done in the right way*. By doing so, we redefine the role of generative models within self-supervised representation learning, revisiting the term ‘generative pre-training’ to establish a focused domain of study. In more detail, we find the following: (1) **corruption and restoration must be applied within the encoder** while training, unlike existing design choices [39, 42], as the encoder is what is ultimately transferred to extract features in downstream tasks; (2) **noise must be added at the feature level**, and is particularly effective when added at lower layers of the encoder, which is where high-frequency details are present; and (3) using both the masking strategy and the noising strategy can interfere with each other and **these strategies must be explicitly disentangled**—we ensure this by suppressing the attention between the two different types of tokens.

With these findings, we design a novel pre-training setup that effectively utilizes both masking and noising. Our approach captures a broader range of frequency information as shown in Fig. 2 and Fig. 3, which enhances transferability across a variety of downstream tasks and benchmarks—

CUB-200-2011 [38], NABirds [35], iNaturalist 2017 [36], iNaturalist 2018 [37], Stanford Cars [20], Aircraft [26], ImageNet [9], ADE20K [44], and COCO [21]—achieving up to an 8.1% gain over MIM methods and an 8.0% improvement over recent generative baselines; see Fig. 1.

To summarize, our contributions are:

- we provide a thorough empirical study on why current noising-based pre-training approaches [39, 42] do not provide noticeable gains for recognition tasks;
- we provide guidelines from our detailed study on how to use noise within pre-training;
- and with our findings, we propose a novel pre-training method that outperforms the state-of-the-art on a wide range of recognition tasks, including fine-grained tasks.

2. Preliminary and Related Works

As the intuitions and the findings behind our work are grounded on masked image modeling (MIM) and denoising diffusion models, we first review them for completeness.

2.1. Masked Image Modeling

The core idea behind MIM is to randomly mask portions of images (tokens) and then learn to reconstruct them in a self-supervised manner.

Random masking. Formally, let $X \in \mathbb{R}^{N \times L \times D}$ repre-

sent an image sequence (tokens), where N denotes the batch size, L is the number of tokens in each image, and D represents the dimension of each token. Let us further denote the mask generation process as $M = \Phi_M(X, \gamma)$, where γ is the masking ratio, and $M \in \{0, 1\}^{N \times L}$ is the mask that is generated. We can then write the remaining visible tokens as $X_{\text{masked}} = M \odot X$, where \odot is the Hadamard product.

Reconstruction. To learn to reconstruct the original tokens X back from only the visible ones X_{vis} , training of MIMs typically relies on mean squared error (MSE). With the token predictions \hat{X} from MIM framework that takes as input the masked visible tokens X_{masked} , we minimize the loss:

$$\mathcal{L}_{\text{MIM}} = \frac{1}{\sum_{k,l} M_{k,l}} \sum_{k=1}^N \sum_{l=1}^L M_{k,l} \|\hat{X}_{k,l} - \bar{X}_{k,l}\|^2, \quad (1)$$

where $\bar{X} = X_{\text{vis}}$.

Recent works. MIM approaches [1, 5, 7, 8, 10, 14, 40, 41] adapt the concept of Masked Language Modeling (MLM) from NLP. BEiT [1] applies MLM-like pre-training to images using discrete visual tokens generated by a pre-trained dVAE. MAE [14] focuses only on visible patches in the encoder, predicting masked pixel values through a decoder. SimMIM [40] uses both visible and masked patches in the encoder and predicts original pixels directly. Recent advances [7, 8] focus on masked tokens for fast convergence and performance improvement.

2.2. Denoising Diffusion Model

Denoising diffusion models are trained by progressively corrupting the input data with additive Gaussian noise, which is then a denoiser is trained to recover the data. This is in a similar spirit to MIMs, but unlike MIMs, the theoretical foundations allow the model to be used to generate completely new data, hence they are generative. [34] Various works [15, 16, 25, 31] have thus sought to utilize diffusion models beyond purely generative applications.

Forward diffusion. Forward diffusion iteratively adds noise to an input image sequence $X \in \mathbb{R}^{N \times L \times D}$ over T time steps. At each time step t , a noise schedule $\beta_t \in \mathbb{R}$ controls the amount of noise added, where β^t is a scalar that determines the noise level at time step t . The corrupted representation X^t at step t is then defined as:

$$X^t = \sqrt{1 - \beta^t} \cdot X^{t-1} + \sqrt{\beta^t} \cdot \epsilon, \quad (2)$$

where $\epsilon \sim \mathcal{N}(\mathbf{0}, \mathbf{I})$ is the Gaussian noise with a zero matrix $\mathbf{0}$ and an identity covariance matrix \mathbf{I} . This iterative process gradually *diffuses* the data towards Gaussian noise as t approaches T .

Denoising. With the corrupted signal, the denoiser then learns to undo this corruption, effectively allowing the

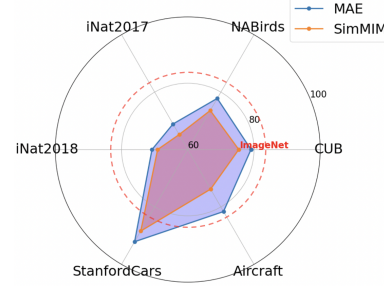


Figure 4. Fine-grained visual categorization (FGVC) is a critical benchmark for evaluating recognition models and require detailed, localized feature learning. However, MIM approaches [14, 40] show limitations on FGVC tasks, with the radar graph revealing substantial room for improvement to reach the ideal boundary and also to the performance on the standard recognition task.

model to traverse back through the diffusion process, that is, transform Gaussian noise to clean data that follows the data distribution. Specifically, starting from X^T , the model learns to predict the clean image X^0 by estimating the intermediate states through a denoising function Φ_{denoise} , which is typically parameterized as a neural network. The denoising step at time t can be represented as:

$$\hat{X}^{t-1} = \Phi_{\text{denoise}}(X^t, t), \quad (3)$$

where \hat{X}^{t-1} represents the denoised estimate at time $t - 1$. Training of $\Phi_{\text{denoise}}(X^t, t)$ is performed through various variations of the original DDIM [34] and DDPM [17] methods, including recent family of Rectified Flow models [22], but are all essentially focusing on obtaining \hat{X}^{t-1} estimates in some form that will accurately lead toward X^0 through various solvers [19, 24].

Recent works. Denoising diffusion models [17, 27, 29, 31, 32] have gained prominence in generative tasks for their ability to produce high-quality, detailed images. DDPM [17] introduced the foundational framework, where Gaussian noise is gradually added to an image and then removed in a reverse process, Improved DDPM [27] enhanced this approach with modifications in noise scheduling and model architecture. LDM [31] further improved efficiency by operating in a compressed latent space rather than pixel space, allowing various practical applications.

2.3. Pre-training via denoising

With preliminaries on MIMs and denoising diffusion models, we now review two representative works that aim to marry the two schools of thought into a single pre-training framework.

DiffMAE. DiffMAE [39] proposes a framework combining diffusion-based generative modeling and MIM. DiffMAE operates by introducing noised tokens instead of masking tokens out. Rather than utilizing a masked token, the

noise is applied to the regions indicated by binary mask $M \in \{0, 1\}^{N \times L}$. Following the noise schedule defined by $\alpha_t \in \mathbb{R}$, Gaussian noise $\epsilon \sim \mathcal{N}(\mathbf{0}, \mathbf{I})$ is applied at each step of the diffusion process. We thus write the noise addition (masking) process as:

$$X \odot (1 - M) + (\sqrt{\alpha_t} \cdot X + \sqrt{1 - \alpha_t} \cdot \epsilon) \odot M, \quad (4)$$

In what follows, for ease in notation, we denote the visible image tokens in X_{masked} , that is, tokens in $X \odot M$ as $x_v \in \mathbb{R}^{N \times D}$ and the noisy tokens, the tokens in $(\sqrt{\alpha_t} \cdot X + \sqrt{1 - \alpha_t} \cdot \epsilon) \odot (1 - M)$ as $x_n \in \mathbb{R}^{N \times D}$. The model then reconstructs X from the corrupted image X_{masked} by denoising the noisy tokens x_n through a reverse process that iteratively refines x_n using visible tokens x_v :

$$\hat{x}_n^{t-1} = \Phi_{\text{denoise}}(x_n^t, x_v, t), \quad (5)$$

where Φ_{denoise} is the denoising function.

MaskDiT. MaskDiT [42] proposes a generative pre-training approach that leverages masked transformers for faster training of diffusion models. Unlike DiffMAE, MaskDiT generates a masked input X_{masked} , using both masked tokens and noised tokens. We describe the noise addition and masking process as:

$$\theta \odot M + (\sqrt{\alpha_t} \cdot X + \sqrt{1 - \alpha_t} \cdot \epsilon) \odot (1 - M), \quad (6)$$

where θ is a parameter for masked tokens, $x_m \in \mathbb{R}^{N \times D}$. Similarly, as before, we denote the masked tokens $\theta \odot M$ of X_{masked} as x_m . Then, the model reconstructs the noise tokens $x_n^t \in \mathbb{R}^{N \times D}$ and masked tokens x_m through a function Φ_{denoise} and $\Phi_{\text{reconstruct}}$:

$$\hat{x}_m^{t-1} = \Phi_{\text{denoise}}(x_n^t, x_v, t) \quad \hat{x} = \Phi_{\text{reconstruct}}(x_m, x_v). \quad (7)$$

3. A Deep Dive into Pre-training Methods

Given the preliminaries, unfortunately, none of the existing works show a clear benefit in combining denoising models with MIM, especially for fine-grained recognition tasks as demonstrated in Figure 1. Before we discuss our method, to motivate our design choices, we investigate the limitations of existing methods and where their potential pitfalls are.

3.1. Limitations of Conventional Methods

We first examine the status of Masked Image Modeling then Denoising-based Pre-training.

Limitations of Masked Image Modeling in Fine-Grained Recognition. Masked Image Modeling (MIM) initially demonstrated strong transferability in downstream tasks like image classification, positioning it as a promising approach for self-supervised learning. Meanwhile, fine-grained recognition tasks, such as fine-grained visual categorization (FGVC), have become essential benchmarks for

recognition models in computer vision due to their need for detailed, localized feature learning to distinguish between highly similar categories. MIM approaches [14, 40] reveal limitations on FGVC tasks, as shown in Figure 4.

Specifically, we pre-trained each MIM method under identical settings and then fine-tuned them on each fine-grained datasets, such as CUB-200-2011 [38], NABirds [35], iNaturalist 2017 [36], iNaturalist 2018 [37], Stanford Cars [20], and Aircraft [26] to obtain the transferred performance. As observed in the radar graph, MIM pre-training alone falls short of achieving high accuracy, and the remaining gap compared to the ideal boundary and the ImageNet baseline (performance on the standard recognition task), highlights significant room for improvement in the FGVC task. One possible reason is that the reconstruction objective MIM relatively focuses on broader, lower-frequency structures as illustrated in Figure 2, which may limit its ability to capture the fine-grained details that are essential to distinguishing across visually similar categories.

Challenges of Recent Denoising-based Pre-Training for Recognition Tasks. Recent denoising-based pre-training approaches [39, 42], which utilize additive noise to denoise masked image modeling, were designed to improve representation learning. To be precise, DiffMAE [39] is designed for both recognition and generative tasks, while MaskDiT [42] focuses specifically on generative tasks. However, our evaluations, along with results reported in the study [42], reveal that these generative methods struggle to deliver notable gains on recognition tasks compared to representative MIM baselines [14, 40].

In Figure 5, we show results of pre-training with recent denoising-based methods, DiffMAE [39] and MaskDiT [42], and MIM baselines, SimMIM [40] and MAE [14]. For a fair comparison, all methods were pre-trained under the same settings and subsequently fine-tuned on each recognition dataset. Notably, recent generative pre-training methods show minimal performance differences from MIM baselines on standard recognition tasks such as ImageNet [9] image classification. It even falls short in capturing the fine-grained features essential for FGVC tasks on datasets such as CUB-200-2011 [38], NABirds [35], iNaturalist 2017 [36], iNaturalist 2018 [37], Stanford Cars [20], and Aircraft [26], where subtle distinctions are crucial. Except for DiffMAE [39], we rely on the official implementation—for DiffMAE, we carefully reimplemented the method based on the manuscript. To ensure transparency, all implemented code is provided in the Supplementary Material. This limitation indicates that simply incorporating a denoising process into MIM pre-training does not inherently elevate the representation quality essential for precise recognition tasks.

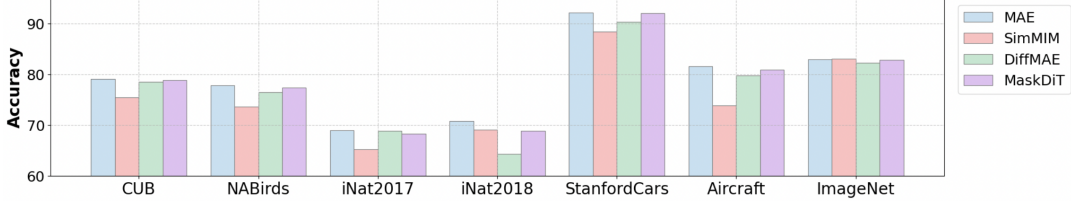


Figure 5. Our evaluations reveal that recent generative pre-training approaches [39, 42] yield limited gains over MIM baselines [14, 40] on recognition tasks, suggesting that simply adding denoising to MIM pre-training does not inherently elevate the representation quality essential for precise recognition. Except for DiffMAE [39], we rely on the official implementation—for DiffMAE, we carefully reimplemented the method based on the manuscript as no code is available. For reproducibility, all implemented code has been included in the Supplementary Material.

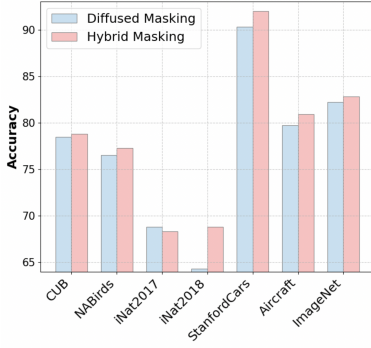


Figure 6. Hybrid masking achieved slightly better performance across datasets, as it consistently retains a fully masked portion that enhances semantic discriminability. In contrast, diffused masking relies on tokens with random noise intensities, which may limit its effectiveness.

3.2. How should noising and masking be combined?

Despite integrating MIM with denoising diffusion models, these methods [39, 42] yield no notable gains over standard MIM approaches [14, 40] on recognition tasks. We first focus on how noising and masking are combined in recent baselines to uncover why they fall short on recognition tasks. Specifically, we look into the two representative cases of integrations, DiffMAE [39] and MaskDiT [42]. We note that these methods represent the two different ways in which noise can be added:

- at visible tokens, *i.e.*, **Diffused Masking** [39]; or
- at masked tokens, *i.e.*, **Hybrid Masking** [42].

Diffused masking employs a noisy, diffused token alongside a clean visible token, as specified in (4). On the other hand, *hybrid masking* utilizes both a masked token and a noisy token, as described in (6). As outlined in Section 2.1, the conventional MIM setup consists of both masked and visible tokens; simply put, diffused masking modifies this by replacing the masked token with a noisy token, while hybrid masking keeps the masked token but adds noise to the visible token. Thus, diffused masking focuses only on denoising, as in (5), while hybrid masking simultaneously performs noised token denoising and masked token recon-

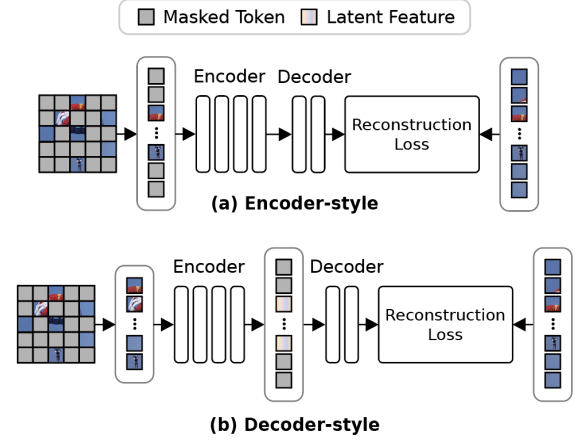


Figure 7. The study of MIM is broadly segmented into two types based on masked token placement: 1) Encoder-style, which reconstructs masked regions within the encoder [1, 40, 41], and 2) Decoder-style, where reconstruction occurs solely in the decoder [5, 10, 14]. The recent generative baselines [39, 42] build on MAE [14], can be seen as decoder-style approaches.

struction, as in (7).

We evaluated these two masking methods used by recent baselines [39, 42] to determine which approach performs better across a wide range of recognition tasks. For a fair comparison, we re-implemented both methods to ensure all conditions other than the masking method—such as model architecture and training schedule—are identical.

Figure 6 presents the transfer learning performance of each masking method, pre-trained on ImageNet-1K [9], and fine-tuned across various recognition tasks and datasets. [9, 20, 26, 35–38] The results indicate that *hybrid masking* achieved slightly better performance across datasets. We attribute this difference to the fact that diffused masking relies solely on noise. Using a random time sampling, when the diffusion noise is weak, the masked image of diffused masking would be very close to the original image, thus rendering the pre-training task trivial—the network will not learn useful semantic representations. In contrast, hybrid masking would always contain masked portions of the im-

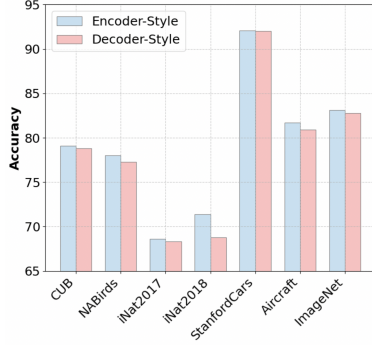


Figure 8. We advocate for an encoder-style approach, as it is the encoder that is transferred for downstream fine-tuning. We implemented two naive frameworks of encoder-style and decoder-style generative frameworks. However, the results showed minimal difference, with the encoder-style performing slightly better. Section 3.4 further explains that a naive implementation of this approach failed to fully leverage its potential.

age, forcing the training objective to solve both denoising and de-masking. In other words, even when the diffusion part is completely ignored, there is room for the MIM objective alone to still teach the model in hybrid masking.

3.3. Where Should Noise be Added?

Beyond the strategy to combine masking and noising, we look also into where noise/mask should be injected. The study of MIM is broadly segmented into two competitive approaches, distinguished by the placement of masked tokens, as illustrated in Figure 7: 1) **Encoder-style** and 2) **Decoder-style**. The encoder-style [1, 40, 41] in Figure 7 (a), incorporates masked tokens *within the encoder*, with the reconstruction of masked regions occurring across the encoder-decoder structure. In contrast, the decoder-style approach [5, 10, 14], illustrated in Figure 7 (b), employs masked tokens solely *within the decoder*, where the primary reconstruction is conducted.

A key structural characteristic of the decoder-style is the clear separation between representation learning and reconstruction tasks. The encoder handles representation learning tasks only from visible tokens, while the decoder focuses on the reconstruction tasks using masked tokens.

The recent generative baselines analyzed in Section 3.2 [39, 42] reconstruct masked or noisy tokens within the decoder, utilizing MAE [14]—a representative decoder-style method of MIM—as their foundation. Thus, these approaches can be regarded as decoder-style approaches, but in the context of generative pre-training.

However, we focus on the fact that it is the encoder that is transferred and utilized for downstream fine-tuning. Therefore, we advocate for an encoder-style approach, adding corruption and focusing reconstruction within the encoder, hypothesizing that this will allow the benefits of noising which could translate to pre-training.

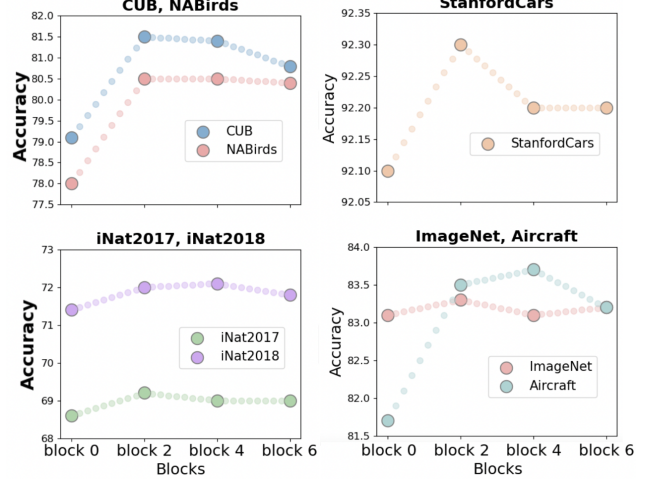


Figure 9. We conducted experiments by introducing noise at various encoder stages (blocks 0, 2, 4, and 6). Results show that adding noise in feature-space (blocks 2, 4, and 6) outperforms pixel-space (block 0) for recognition tasks, with optimal performance at block 2, where high-frequency details are captured.

To support this hypothesis, we implemented two naive generative frameworks featuring hybrid masking strategies that differ only in their placement of corruption. We kept all other factors identical. We then evaluated their performance on transfer learning by pre-training both models on ImageNet-1K [9] and fine-tuning them on the range of recognition tasks and datasets.

Figure 8 illustrates the transfer learning performance of each masking method. Contrary to our hypothesis, the results revealed minimal performance difference between the two structures. To be specific, in both fine-grained and standard recognition tasks, the difference between the two architectures was minimal, with the encoder-style structure performing only slightly better. As we will discuss in Section 3.4, this, in fact, is because naively implementing this idea does not show its true potential.

3.4. Method

The encoder-style framework implemented in the above Section 3.3 is a naive and straightforward approach, as we simply shifted the corruption process to the start of the encoder. To properly introduce an encoder-style framework, we analyzed the structural differences between encoder-style and decoder-style approaches and found two key aspects for consideration:

- **Feature-level noise addition:** noise should be added at the feature level; and
- **Task disentanglement:** the processes of denoising and mask reconstructing should be explicitly disentangled.

Feature-level noise addition. Much of the success of denoising diffusion models is rooted in the application of

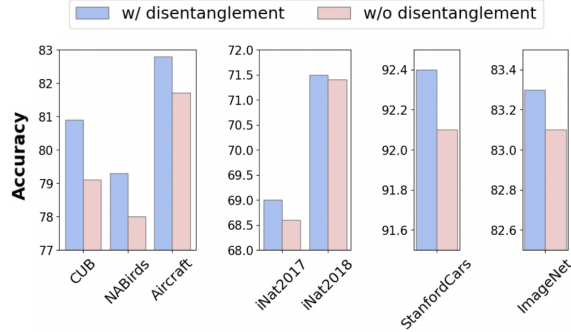


Figure 10. We propose an explicit objective to disentangle the de-masking task from the de-noising task, fully harnessing both reconstructions within the encoder. The disruption loss adjusts the weight distribution of the affinity map, minimizing the influence of masked tokens on noisy visible tokens, and enhancing performance across both fine-grained and standard recognition tasks.

noise at the latent (feature) space [6, 31]. While pixel-space diffusion exists [18], they need careful strategies on how noise should be applied. As such, we also suspect this to be the case for pre-training. However, in the naive implementation that we consider in Section 3.3, the decoder-style method adds noise at the latent space immediately before the decoder, whereas the encoder-style approach injects noise in pixel-space, prior to the encoder. We thus experimented with adding noise to various blocks within the encoder to investigate the impact of different noise-addition locations.

In Figure 9, we conducted experiments by varying the stage at which noise is introduced within the encoder, specifically at different encoder blocks (blocks 0, 2, 4, and 6). The transfer learning performance results for recognition tasks verify that adding noise in feature-space (blocks 2, 4, and 6) is more effective than in pixel-space (block 0). Additionally, the highest performance observed at ‘encoder block 2’ suggests that noise addition is particularly effective when applied in the lower layers of the encoder, where high-frequency details are captured. This result reveals that the injecting noise at the feature level is crucial for maximizing the transfer learning potential of the model.

Task disentanglement. Referring to recent studies of MIM [7, 10, 14], encoder-style approaches often underperform compared to decoder-style approaches. This is primarily because masked tokens are trained in a direction orthogonal to that of visible tokens [7], which can interfere with the encoding process of visible tokens. Because we maintain the structure of hybrid masking, based on the results of Section 3.2, we suspect this issue to also arise for generative pre-training with denoising models. Specifically, masked tokens may disrupt the encoding process of noisy visible tokens.

The decoder-style approach [5, 10, 14] avoids this issue

by assigning distinct tasks to the encoder and decoder, focusing the encoder on representation learning and the decoder on masked token reconstruction. However, as we wish to apply them both to the encoder, it is essential to explicitly disentangle these two within the encoder itself.

To address this, we propose an explicit objective that disentangles the de-masking strategy from the de-noising strategy. We introduce disruption loss, a variant of masked token optimization proposed in MTO [7], designed to suppress attention between the two different token types. Disruption loss leverages per-row sparsities within the affinity matrix, which consists of four quadrants as follows:

$$A = \begin{bmatrix} A_{vv} & A_{vm} \\ A_{mv} & A_{mm} \end{bmatrix}, \quad (8)$$

where A_{vv} represents weights between visible-visible tokens, A_{vm} and A_{mv} represents affinities between visible-masked tokens, and A_{mm} represents weights among masked tokens. The disruption loss \mathcal{L}_d recalibrates the weight distribution of A , minimizing the impact of masked tokens x_m on noisy visible tokens x_n^t :

$$\mathcal{L}_d = - \sum_{i \in \mathcal{N}} \sum_j \tilde{p}_{i,j} \log \tilde{p}_{i,j} \quad (9)$$

where \mathcal{N} denotes the index set of noisy visible tokens x_n^t , and \tilde{p} is an element of A , satisfying $0 < \tilde{p}_{i,j} < 1$ and $\sum_j \tilde{p}_{i,j} = 1$. The application of \mathcal{L}_d reduces interference between different token types and thus ensures effective task disentanglement between denoising and mask reconstruction within the encoder.

The experimental results in Figure 10 show a performance improvement with this weight adjustment in both fine-grained and standard recognition tasks. Thus, disentangling the de-masking and de-noising strategies through explicit task disentanglement maximizes the transfer potential of the encoder-style approach.

Through these findings, we demonstrate that the encoder-style approach can indeed outperform the decoder-style in generative pre-training frameworks.

4. Experiments

4.1. Implementation Detail

All experiments in this manuscript were conducted under precisely identical conditions to ensure accurate analysis. To achieve this consistency, we implemented each method, so reported results may differ from original papers. All experiments used ViT-B [11] as the backbone architecture applying a unified 400-epoch training schedule on our hardware configuration (4 × A100 GPUs). Pre-training was performed on the ImageNet-1K [9] classification dataset, followed by fine-tuning on respective down-

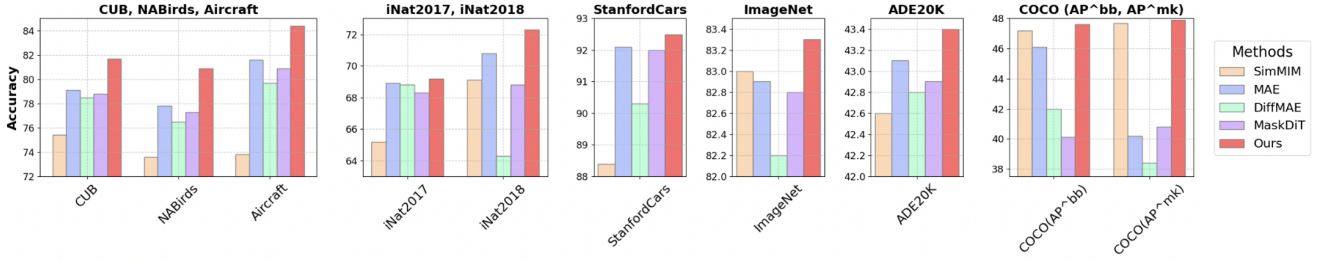


Figure 11. The proposed method (Ours) consistently outperforms representative MIM [14, 40] and generative methods [39, 42] across a wide range of recognition tasks, capturing diverse frequency details as shown in Fig. 2 and Fig. 3, that improve accuracy in FGVC, image classification, semantic segmentation, object detection, and instance segmentation tasks.

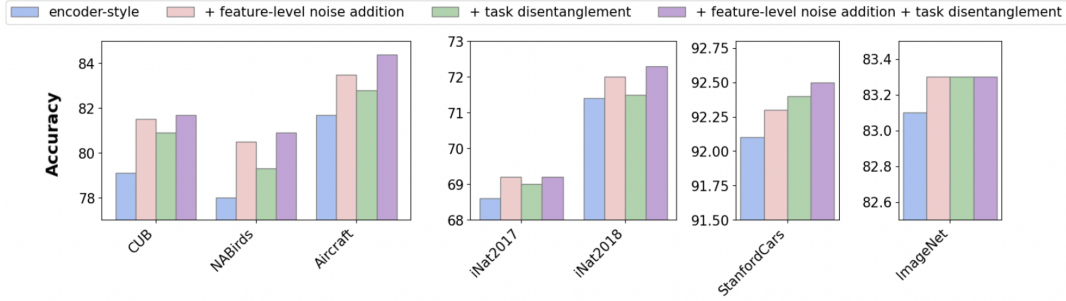


Figure 12. We present the ablation study results on the components of the proposed method. Feature-level noise addition and task disentanglement together yield the best results, highlighting the importance of these structural considerations in improving transferability on both fine-grained and standard recognition tasks.

stream task datasets. For transparency, all code, parameters, and detailed experimental settings are available in the Supplementary Material.

4.2. Main Result

In Figure 11, we evaluate the proposed method on diverse tasks, including fine-grained visual categorization (FGVC), image classification, semantic segmentation, object detection, and instance segmentation, each with task-specific datasets. FGVC datasets (CUB-200-2011 [38], NABirds [35], iNaturalist 2017 [36], iNaturalist 2018 [37], Stanford Cars [20], Aircraft [26]) demand detailed, fine-grained feature learning to distinguish visually similar classes. In contrast, standard recognition tasks (ImageNet [9]), semantic segmentation (ADE20K [44]), object detection and instance segmentation (COCO [21]) emphasize broader spatial details at different levels of granularity.

The proposed method (Ours) consistently outperforms representative MIM [14, 40] and generative methods [39, 42] across tasks. In FGVC tasks, our method effectively captures high-frequency, localized features, as shown in Figure 2 and Figure 3, surpassing comparison methods in accuracy. Even in standard recognition tasks, where spatial detail is key, our method shows favourable gains, highlighting that task disentanglement and feature-space noise injection enhance transfer potential and capture diverse frequency information, as demonstrated in Figure 2.

4.3. Ablation on Components

Figure 12 shows the ablation study results on our proposed method, progressively enhanced by feature-level noise addition and task disentanglement, individually and in combination, across various recognition benchmarks.

Feature-level noise consistently improves accuracy in both fine-grained (CUB, NABirds, Aircraft, iNat2017, iNat2018, StanfordCars) and standard recognition tasks (ImageNet). Task disentanglement further enhances performance by separating de-masking and de-noising processes. The combination of both techniques yields the best results. This result underscores the importance of structural design considerations for optimal transfer learning. Further ablation studies are available in the Supplementary Material.

5. Conclusion

We have analyzed why current noising-based pre-training struggles with recognition tasks and provided architectural guidelines. By applying our findings, we achieve notable improvements over existing MIM and other generative approaches.

Limitations and future work. Our analysis is currently limited to recognition tasks. It would thus be interesting to broaden the scope of our study to other applications.

References

- [1] Hangbo Bao, Li Dong, Songhao Piao, and Furu Wei. Beit: Bert pre-training of image transformers. In *International Conference on Learning Representations*, 2021. 1, 3, 5, 6
- [2] Nicolas Carion, Francisco Massa, Gabriel Synnaeve, Nicolas Usunier, Alexander Kirillov, and Sergey Zagoruyko. End-to-end object detection with transformers. In *European conference on computer vision*, pages 213–229. Springer, 2020. 1
- [3] Hanting Chen, Yunhe Wang, Tianyu Guo, Chang Xu, Yiping Deng, Zhenhua Liu, Siwei Ma, Chunjing Xu, Chao Xu, and Wen Gao. Pre-trained image processing transformer. In *Proceedings of the IEEE/CVF conference on computer vision and pattern recognition*, pages 12299–12310, 2021. 1
- [4] Ting Chen, Simon Kornblith, Mohammad Norouzi, and Geoffrey Hinton. A simple framework for contrastive learning of visual representations. In *International conference on machine learning*, pages 1597–1607. PMLR, 2020. 1
- [5] Xiaokang Chen, Mingyu Ding, Xiaodi Wang, Ying Xin, Shentong Mo, Yunhao Wang, Shumin Han, Ping Luo, Gang Zeng, and Jingdong Wang. Context autoencoder for self-supervised representation learning. *International Journal of Computer Vision*, 132(1):208–223, 2024. 3, 5, 6, 7
- [6] Xinlei Chen, Zhuang Liu, Saining Xie, and Kaiming He. Deconstructing denoising diffusion models for self-supervised learning. *arXiv preprint arXiv:2401.14404*, 2024. 7
- [7] Hyesong Choi, Hunsang Lee, Seyoung Joung, Hyejin Park, Jiyeong Kim, and Dongbo Min. Emerging property of masked token for effective pre-training. *arXiv preprint arXiv:2404.08330*, 2024. 3, 7
- [8] Hyesong Choi, Hyejin Park, Kwang Moo Yi, Sungmin Cha, and Dongbo Min. Saliency-based adaptive masking: revisiting token dynamics for enhanced pre-training. In *European Conference on Computer Vision*, pages 343–359. Springer, 2025. 3
- [9] Jia Deng, Wei Dong, Richard Socher, Li-Jia Li, Kai Li, and Li Fei-Fei. Imagenet: A large-scale hierarchical image database. In *2009 IEEE conference on computer vision and pattern recognition*, pages 248–255. Ieee, 2009. 1, 2, 4, 5, 6, 7, 8
- [10] Xiaoyi Dong, Jianmin Bao, Ting Zhang, Dongdong Chen, Weiming Zhang, Lu Yuan, Dong Chen, Fang Wen, and Nenghai Yu. Bootstrapped masked autoencoders for vision bert pretraining. In *European Conference on Computer Vision*, pages 247–264. Springer, 2022. 3, 5, 6, 7
- [11] Alexey Dosovitskiy, Lucas Beyer, Alexander Kolesnikov, Dirk Weissenborn, Xiaohua Zhai, Thomas Unterthiner, Mostafa Dehghani, Matthias Minderer, Georg Heigold, Sylvain Gelly, et al. An image is worth 16x16 words: Transformers for image recognition at scale. *arXiv preprint arXiv:2010.11929*, 2020. 1, 7
- [12] Jean-Bastien Grill, Florian Strub, Florent Altché, Corentin Tallec, Pierre Richemond, Elena Buchatskaya, Carl Doersch, Bernardo Avila Pires, Zhaohan Guo, Mohammad Gheshlaghi Azar, et al. Bootstrap your own latent-a new approach to self-supervised learning. *Advances in neural information processing systems*, 33:21271–21284, 2020. 1
- [13] Kaiming He, Haoqi Fan, Yuxin Wu, Saining Xie, and Ross Girshick. Momentum contrast for unsupervised visual representation learning. In *Proceedings of the IEEE/CVF conference on computer vision and pattern recognition*, pages 9729–9738, 2020.
- [14] Kaiming He, Xinlei Chen, Saining Xie, Yanghao Li, Piotr Dollár, and Ross Girshick. Masked autoencoders are scalable vision learners. In *Proceedings of the IEEE/CVF Conference on Computer Vision and Pattern Recognition*, pages 16000–16009, 2022. 1, 3, 4, 5, 6, 7, 8
- [15] Eric Hedlin, Gopal Sharma, Shweta Mahajan, Xingzhe He, Hossam Isack, Abhishek Kar, Helge Rhodin, Andrea Tagliasacchi, and Kwang Moo Yi. Unsupervised keypoints from pretrained diffusion models. In *Proceedings of the IEEE/CVF Conference on Computer Vision and Pattern Recognition*, pages 22820–22830, 2024. 3
- [16] Eric Hedlin, Gopal Sharma, Shweta Mahajan, Hossam Isack, Abhishek Kar, Andrea Tagliasacchi, and Kwang Moo Yi. Unsupervised semantic correspondence using stable diffusion. *Advances in Neural Information Processing Systems*, 36, 2024. 3
- [17] Jonathan Ho, Ajay Jain, and Pieter Abbeel. Denoising diffusion probabilistic models. *Advances in neural information processing systems*, 33:6840–6851, 2020. 3
- [18] Emiel Hooeboom, Thomas Mensink, Jonathan Heek, Kay Lamerigts, Ruiqi Gao, and Tim Salimans. Simpler diffusion (sid2): 1.5 fid on imagenet512 with pixel-space diffusion. *arXiv preprint arXiv:2410.19324*, 2024. 7
- [19] Tero Karras, Miika Aittala, Timo Aila, and Samuli Laine. Elucidating the design space of diffusion-based generative models. *Advances in neural information processing systems*, 35:26565–26577, 2022. 3
- [20] Jonathan Krause, Michael Stark, Jia Deng, and Li Fei-Fei. 3d object representations for fine-grained categorization. In *Proceedings of the IEEE international conference on computer vision workshops*, pages 554–561, 2013. 1, 2, 4, 5, 8
- [21] Tsung-Yi Lin, Michael Maire, Serge Belongie, James Hays, Pietro Perona, Deva Ramanan, Piotr Dollár, and C Lawrence Zitnick. Microsoft coco: Common objects in context. In *Computer Vision—ECCV 2014: 13th European Conference, Zurich, Switzerland, September 6–12, 2014, Proceedings, Part V 13*, pages 740–755. Springer, 2014. 1, 2, 8
- [22] Xingchao Liu, Chengyue Gong, and Qiang Liu. Flow straight and fast: Learning to generate and transfer data with rectified flow. *arXiv preprint arXiv:2209.03003*, 2022. 3
- [23] Ze Liu, Yutong Lin, Yue Cao, Han Hu, Yixuan Wei, Zheng Zhang, Stephen Lin, and Baining Guo. Swin transformer: Hierarchical vision transformer using shifted windows. In *Proceedings of the IEEE/CVF international conference on computer vision*, pages 10012–10022, 2021. 1
- [24] Cheng Lu, Yuhao Zhou, Fan Bao, Jianfei Chen, Chongxuan Li, and Jun Zhu. Dpm-solver: A fast ode solver for diffusion probabilistic model sampling in around 10 steps. *Advances in Neural Information Processing Systems*, 35:5775–5787, 2022. 3
- [25] Grace Luo, Lisa Dunlap, Dong Huk Park, Aleksander Holynski, and Trevor Darrell. Diffusion hyperfeatures: Searching

- through time and space for semantic correspondence. *Advances in Neural Information Processing Systems*, 36, 2024. 3
- [26] Subhransu Maji, Esa Rahtu, Juho Kannala, Matthew Blaschko, and Andrea Vedaldi. Fine-grained visual classification of aircraft. *arXiv preprint arXiv:1306.5151*, 2013. 1, 2, 4, 5, 8
- [27] Alexander Quinn Nichol and Prafulla Dhariwal. Improved denoising diffusion probabilistic models. In *International conference on machine learning*, pages 8162–8171. PMLR, 2021. 3
- [28] Alec Radford, Jong Wook Kim, Chris Hallacy, Aditya Ramesh, Gabriel Goh, Sandhini Agarwal, Girish Sastry, Amanda Askell, Pamela Mishkin, Jack Clark, et al. Learning transferable visual models from natural language supervision. In *International conference on machine learning*, pages 8748–8763. PMLR, 2021. 1
- [29] Aditya Ramesh, Mikhail Pavlov, Gabriel Goh, Scott Gray, Chelsea Voss, Alec Radford, Mark Chen, and Ilya Sutskever. Zero-shot text-to-image generation. In *International conference on machine learning*, pages 8821–8831. Pmlr, 2021. 1, 3
- [30] René Ranftl, Alexey Bochkovskiy, and Vladlen Koltun. Vision transformers for dense prediction. In *Proceedings of the IEEE/CVF international conference on computer vision*, pages 12179–12188, 2021. 1
- [31] Robin Rombach, Andreas Blattmann, Dominik Lorenz, Patrick Esser, and Björn Ommer. High-resolution image synthesis with latent diffusion models. In *Proceedings of the IEEE/CVF conference on computer vision and pattern recognition*, pages 10684–10695, 2022. 1, 3, 7
- [32] Chitwan Saharia, William Chan, Saurabh Saxena, Lala Li, Jay Whang, Emily L Denton, Kamyar Ghasemipour, Raphael Gontijo Lopes, Burcu Karagol Ayan, Tim Salimans, et al. Photorealistic text-to-image diffusion models with deep language understanding. *Advances in neural information processing systems*, 35:36479–36494, 2022. 1, 3
- [33] Christoph Schuhmann, Richard Vencu, Romain Beaumont, Robert Kaczmarczyk, Clayton Mullis, Aarush Katta, Theo Coombes, Jenia Jitsev, and Aran Komatsuzaki. Laion-400m: Open dataset of clip-filtered 400 million image-text pairs. *arXiv preprint arXiv:2111.02114*, 2021. 1
- [34] Jiaming Song, Chenlin Meng, and Stefano Ermon. Denoising diffusion implicit models. *arXiv preprint arXiv:2010.02502*, 2020. 3
- [35] Grant Van Horn, Steve Branson, Ryan Farrell, Scott Haber, Jessie Barry, Panos Ipeirotis, Pietro Perona, and Serge Belongie. Building a bird recognition app and large scale dataset with citizen scientists: The fine print in fine-grained dataset collection. In *Proceedings of the IEEE conference on computer vision and pattern recognition*, pages 595–604, 2015. 1, 2, 4, 5, 8
- [36] Grant Van Horn, Oisín Mac Aodha, Yang Song, Alexander Shepard, Hartwig Adam, Pietro Perona, and Serge Belongie. The inaturalist challenge 2017 dataset. *arXiv preprint arXiv:1707.06642*, 1(2):4, 2017. 2, 4, 8
- [37] Grant Van Horn, Oisín Mac Aodha, Yang Song, Yin Cui, Chen Sun, Alex Shepard, Hartwig Adam, Pietro Perona, and Serge Belongie. The inaturalist species classification and detection dataset. In *Proceedings of the IEEE conference on computer vision and pattern recognition*, pages 8769–8778, 2018. 2, 4, 8
- [38] Catherine Wah, Steve Branson, Peter Welinder, Pietro Perona, and Serge Belongie. The caltech-ucsd birds-200-2011 dataset. 2011. 1, 2, 4, 5, 8
- [39] Chen Wei, Kartikeya Mangalam, Po-Yao Huang, Yanghao Li, Haoqi Fan, Hu Xu, Huiyu Wang, Cihang Xie, Alan Yuille, and Christoph Feichtenhofer. Diffusion models as masked autoencoders. In *Proceedings of the IEEE/CVF International Conference on Computer Vision*, pages 16284–16294, 2023. 1, 2, 3, 4, 5, 6, 8
- [40] Zhenda Xie, Zheng Zhang, Yue Cao, Yutong Lin, Jianmin Bao, Zhuliang Yao, Qi Dai, and Han Hu. Simmim: A simple framework for masked image modeling. In *Proceedings of the IEEE/CVF Conference on Computer Vision and Pattern Recognition*, pages 9653–9663, 2022. 1, 2, 3, 4, 5, 6, 8
- [41] Kun Yi, Yixiao Ge, Xiaotong Li, Shusheng Yang, Dian Li, Jianping Wu, Ying Shan, and Xiaohu Qie. Masked image modeling with denoising contrast. *arXiv preprint arXiv:2205.09616*, 2022. 3, 5, 6
- [42] Hongkai Zheng, Weili Nie, Arash Vahdat, and Anima Anandkumar. Fast training of diffusion models with masked transformers. *arXiv preprint arXiv:2306.09305*, 2023. 1, 2, 4, 5, 6, 8
- [43] Sixiao Zheng, Jiachen Lu, Hengshuang Zhao, Xiatian Zhu, Zekun Luo, Yabiao Wang, Yanwei Fu, Jianfeng Feng, Tao Xiang, Philip HS Torr, et al. Rethinking semantic segmentation from a sequence-to-sequence perspective with transformers. In *Proceedings of the IEEE/CVF conference on computer vision and pattern recognition*, pages 6881–6890, 2021. 1
- [44] Bolei Zhou, Hang Zhao, Xavier Puig, Sanja Fidler, Adela Barriuso, and Antonio Torralba. Scene parsing through ade20k dataset. In *Proceedings of the IEEE conference on computer vision and pattern recognition*, pages 633–641, 2017. 1, 2, 8
- [45] Xizhou Zhu, Weijie Su, Lewei Lu, Bin Li, Xiaogang Wang, and Jifeng Dai. Deformable detr: Deformable transformers for end-to-end object detection. *arXiv preprint arXiv:2010.04159*, 2020. 1